VOLUME 122, NUMBER 28
JULY 19, 2000

JOURNAL OF THE AMERICAN CHEMICAL SOCIETY

Transition-State Analysis for Depurination of DNA by Ricin A-Chain

Xiang-Yang Chen,[‡] Paul J. Berti,[§] and Vern L. Schramm*

Contribution from the Department of Biochemistry, Albert Einstein College of Medicine, 1300 Morris Park Avenue, Bronx, New York 10461

Received August 2, 1999

Abstract: Ricin toxin A-chain (RTA) exerts its cytotoxicity by depurinating 28 S ribosomal RNA at ribonucleotide A4234, a site of eukaryotic elongation factor binding. Small stem-loop RNAs and DNAs can also be depurinated at the first adenine residue of 5′-GAGA-3′ tetraloops. DNA oligonucleotides were synthesized with DNA polymerase, using dATP labeled with [1′-^{14}C], [5′-^{14}C,9-^{15}N], [1′-^{3}H], [2′R-^{3}H], [2′S-^{3}H] or [5′-^{3}H]. Kinetic isotope effects (KIEs) were measured for depurination of a stem-loop DNA, called dA-10, with the sequence d(5′-GGCGAGAGCC-3′). The commitment to catalysis was measured and found to be negligible, indicating that the experimental KIEs are the intrinsic KIEs of the chemical steps. The experimental KIEs, especially the small primary 1′-^{14}C KIE of 1.015 ± 0.001, demonstrated that the reaction proceeds through a stepwise D_N*A_N mechanism, forming a discrete oxocarbenium·RTA complex with a lifetime $\geq 10^{-12}$ s. The secondary KIEs at 1′-^{3}H, 2′R-^{3}H, and 2′S-^{3}H were large and normal, supporting the existence of an oxocarbenium ion. In a stepwise mechanism, the KIEs are a function of the partitioning of the oxocarbenium ion intermediate forward to products or back to reactants. KIEs calculated from density functional theory (DFT) optimized structures to quantitate partitioning of the intermediate were similar to each other and could not be used to determine partitioning from the experimental KIEs. The large 2′R-^{3}H and 2′S-^{3}H KIEs demonstrate that the ribosyl ring in the oxocarbenium ion adopts a conformation giving maximal hyperconjugative stabilization of the cationic center at C1′. This is in contrast to the RNA substrate where the nucleotide backbone constrains the ribosyl ring in a 3′-endo conformation with little hyperconjugation (Chen, X.-Y.; Berti, P. J.; Schramm, V. L. *J. Am. Chem. Soc.* **2000**, *122*, 1609−1617). The transition state for RNA hydrolysis by RTA is dominated by stem-loop geometry while that for DNA permits hyperconjugative stabilization to determine the transition-state geometry.

Introduction

Ricin A-chain (RTA) catalyzes depurination of synthetic stem-loop RNA and DNA molecules possessing a 5′-GAGA-3′ tetraloop structure.[1−5] The transition state of RNA depurination has been characterized using kinetic isotope effects (KIEs) measured for RNAs isotopically labeled at the depurination site.[6] The reaction involves formation of an enzyme·oxocarbenium ion intermediate, followed by an isotopically insensitive step, such as an enzymatic or substrate conformational change, which is rate-limiting. The rapid attack of water completes depurination. The discovery that RTA depurinates stem-loop DNA

* Corresponding author. Telephone (718) 430-2813. Fax (718) 430-8565. E-mail:vern@aecom.yu.edu.
‡ Present address: Monsanto Company, 800 N. Lindberg Blvd., Mail Zone Q3A, St. Louis, MO 63167.
§ Present address: Department of Chemistry, McMaster University, Hamilton, Ontario, L8S 4M1, Canada.

(1) Endo, Y.; Chan, Y. L.; Lin, A.; Tsurugi, K.; Wool, I. G. *J. Biol. Chem.* **1988**, *263*, 7917−7920.
(2) Endo, Y.; Glück, A.; Wool, I. G. *J. Mol. Biol.* **1991**, *221*, 193−207.
(3) Gluck, A.; Endo, Y.; Wool, I. G. *J. Mol. Biol.* **1992**, *226*, 411−424.
(4) Link, T.; Chen, X.-Y.; Niu, L.-H.; Schramm, V. L. *Toxicon* **1996**, *34*, 1317−1324.
(5) Chen, X. Y.; Link, T. M.; Schramm, V. L. *Biochemistry* **1998**, *37*, 11605−11613.
(6) Chen, X.-Y.; Berti, P. J.; Schramm, V. L. *J. Am. Chem. Soc.* **2000**, *122*, 1609−1617.

10.1021/ja992751a CCC: $19.00
Published on Web 06/27/2000

permits a comparison of transition states for RNA and DNA depurination. The presence of the proR and proS hydrogens at C2′ in 2′-deoxyribose permits the measurement of stereospecific isotope effects to provide further information on ribosyl ring conformation at the transition state.

To better understand the mechanisms of catalytic enhancement, the transition states for the enzymatic and nonenzymatic reactions have been compared. Differences between the transition states reflect how the enzyme alters the intrinsic free energy profile of the reaction in order to promote catalysis. In the case of RTA, comparison with the identical nonenzymatic reaction is not possible because a single base cannot be specifically hydrolyzed nonenzymatically from a 10-mer oligonucleotide. However, the transition state has been reported for a chemically related reaction, the acid-catalyzed hydrolysis of AMP.[7] In the work described here, we have measured KIEs for an alternate substrate of RTA, a DNA 10-mer having the same purine base sequence as the RNA substrate examined previously.[6] Because the DNA reaction mechanism does not involve the rate-limiting conformational change found in the RNA depurination reaction,[6] the experimental KIEs provide direct information on the chemical steps of this $D_N{*}A_N$ (S_N1) mechanism. In addition, the oxocarbenium ion conformation with the DNA substrate suggests that the unusual 3′-endo conformation adopted by the RNA substrate is a result of the conformational preferences of the RNA substrate, rather than being imposed by the enzyme on the substrate.

KIEs are defined as the ratio of rate constants ($^{light}k/^{heavy}k$) for identical reactions except that different isotopes of a specific atom are present in the reactant molecules. KIEs reflect the change in the vibrational environment between the reactant and the transition state of the reaction.[8] That is, they report on changes in the strength of the bonding forces in a molecule. For example, if a given bond becomes longer and weaker at the transition state than in the reactant, the decreased bond stretching forces will lead to a looser vibrational environment and a normal KIE ($^{light}k/^{heavy}k > 1.0$). Conversely, an inverse KIE ($^{light}k/^{heavy}k < 1.0$) results from a bond becoming stronger at the transition state. KIEs also reflect changes in the forces controlling bond bending, torsions and out-of-plane bending. Using substrate molecules isotopically labeled at multiple sites, KIEs can be measured and analyzed to give the transition-state structure in atomic detail. Transition-state structures provide information important for understanding enzyme catalysis and have proven useful in the design of inhibitory molecules that resemble enzymatic transition states.[9−12]

Materials and Methods

Materials. Ricin A-chain (RTA) was purchased from Inland Laboratories (Austin, TX). Myokinase (AK), pyruvate kinase (PK), and coenzyme B_{12} (5′-deoxyadenosylcobalamine) were obtained from Sigma Chemical Co. (St. Louis, MO). Calf intestinal phosphatase (CIP) was obtained from Promega (Madison, WI). 3′-5′ Exonuclease-deficient mutant of Klenow fragment of DNA polymerase I was from US Biochemical (Cleveland, OH). Nuclease P1 and snake venom phosphodiesterase (SVP) were from Pharmacia Biotech (Piscataway, NJ). [2′R-^{3}H]Deoxyadenosine was the generous gift of Dr. Hiromi Morimoto of the National Tritium Labeling Facility at Lawrence Berkeley Laboratory. Ribonucleoside triphosphate reductase (RTPR) was purified from an overexpressing strain of *Escherichia coli*, the generous gift of Prof. Joanne Stubbe of the Massachusetts Institute of Technology.[13] Adenosine kinase was partially purified from calf liver.[14]

Synthesis of Isotopically Labeled ATP. ATP isotopically labeled at specific sites was prepared enzymatically from appropriately ^{3}H-, ^{14}C-, or ^{15}N-labeled glucose, ribose 5-phosphate, and adenine, according to published procedures.[15,16] Labeled ATP was isolated by C18 reversed-phase HPLC eluting with 50 mM triethylammonium acetate (TEAA, pH 6.0) containing 5% methanol.

Synthesis of Isotopically Labeled dATP. A solution containing 50 mM potassium phosphate (pH 7.7), 100 mM sodium acetate (pH 7.2), 5 mM $MgCl_2$, 10 mM phosphoenolpyruvate (PEP), 0.5 mM unlabeled ATP, isotopically labeled ATP, 5 U/mL myokinase, and 10 U/mL pyruvate kinase was incubated at 37 °C for 1 h. To this mixture was added 25 mM DTT, 1 U/μL ribonucleoside triphosphate reductase, and 20 μM coenzyme B_{12} under Ar in the dark. Incubation was continued at 37 °C for additional 2 to 3 h, and then stopped by heating at 95 °C for 2 to 3 min. Labeled dATP was isolated by C18 reversed-phase HPLC, with isocratic elution in 50 mM TEAA (pH 6.0) containing 5% methanol.

Synthesis of [2′R-^{3}H]dATP. To a 200 μL solution containing 50 mM potassium phosphate (pH 7.7), 5 mM $MgCl_2$, 0.5 mM ATP, 10 μM 2′-deoxycoformycin, 5 mM phosphoenolpyruvate (PEP), 0.5 mM 2′-deoxyadenosine, [2′R-^{3}H]deoxyadenosine, 1 U myokinase, and 2 U pyruvate kinase was added 0.2 U partially purified adenosine kinase. Phosphorylation was allowed to proceed for 2 h at 37 °C, and then stopped by heating at 95 °C for 2 to 3 min. The labeled dATP was isolated by C18 reversed-phase HPLC, eluting with 50 mM TEAA (pH 6.0) containing 5% methanol.

Synthesis of Isotopically Labeled Stem-Loop DNA 10-mer: dA-10, [(5′-d(GGCGAGAGCC)-3′]. The labeled DNA was enzymatically synthesized by a DNA polymerase-catalyzed primer extension reaction[17] in a 1 mL solution containing 10 mM Tris·HCl (pH 7.5), 5 mM $MgCl_2$, 50 μM hairpin primer-template, 3 mM dGTP, 3 mM dCTP, 50 μM dATP, approximately 10^7 cpm each of appropriately ^{14}C- and ^{3}H-labeled dATPs, and 100 U of 3′-5′ exonuclease-deficient mutant of Klenow fragment of DNA polymerase I. The hairpin primer-template consisted of 2′-deoxynucleotides at all positions except a ribonucleotide (U) at its 3′-terminus. After incubation at 37 °C overnight, 0.3 M NaOH was added to the mixture and the separation of dA-10 product from hairpin primer-template was allowed to proceed at 55 °C for 2 h by base-catalyzed hydrolysis of the U−G phosphodiester bond. Cleavage occurred only at the uridine site as a result of the neighboring 2′-hydroxyl group. The resulting mixture was then neutralized by addition of 0.36 M HOAc, and the DNAs were precipitated by 2.5 volumes of ethanol. The labeled dA-10 and the hairpin primer-template were separated by 24% denaturing PAGE in 7 M urea, located by UV-shadowing, eluted into 1 M NH_4OAc,[18] and desalted on C18 Sep-Pak columns from Waters (Milford, MA). The hairpin primer-template was dephosphorylated by treatment with alkaline phosphatase and reused.

Synthesis of d(5′-GGCGdRGAGCC-3′) for Second Site Depurination Studies. A depurinated DNA (dR-10) was synthesized on the 1 μmol scale in Trityl-off mode with an ABI 391 DNA synthesizer using standard phosphoramidite chemistry. All reagents and protected deoxynucleoside phosphoramidite monomers including 1,2-dideoxyri-

(7) Mentch, F.; Parkin, D. W.; Schramm, V. L. *Biochemistry* **1987**, *26*, 921−930.
(8) Huskey, W. P. In *Enzyme mechanism from isotope effects*; Cook, P. F., Ed.; CRC Press: Boca Raton, FL., 1991; pp 37−72.
(9) Miles, R. W.; Tyler, P. C.; Furneaux, R. H.; Bagdassarian, C. K.; Schramm, V. L. *Biochemistry* **1998**, *37*, 8615−8621.
(10) Boutellier, M.; Horenstein, B. A.; Semenyaka, A.; Schramm, V. L.; Ganem, B. *Biochemistry* **1994**, *33*, 3994−4000.
(11) Horenstein, B. A.; Zabinski, R. F.; Schramm, V. L. *Tetrahedron Lett.* **1993**, *34*, 7213−7216.
(12) Horenstein, B. A.; Schramm, V. L. *Biochemistry* **1993**, *32*, 7089−7097.
(13) Booker, S.; Stubbe, J. *Proc. Natl. Acad. Sci. U.S.A.* **1993**, *90*, 8352−8356.
(14) Merkler, D. J.; Schramm, V. L. *Anal. Biochem.* **1987**, *167*, 148−153.
(15) Rising, K. A.; Schramm, V. L. *J. Am. Chem. Soc.* **1994**, *116*, 6531−6536.
(16) Parkin, D. W.; Leung, H. B.; Schramm, V. L. *J. Biol. Chem.* **1984**, *259*, 9411−9417.
(17) Zimmer, D. P.; Crothers, D. M. *Proc. Natl. Acad. Sci. U.S.A.* **1995**, *92*, 3091−3095.
(18) Damha, M. J.; Ogilvie, K. K. In *Protocols for Oligonucleotides and Analogues: Synthesis and Properties*; Agrawal, S., Ed.: Humana Press: Totowa, NJ, 1993; pp 81−114.

bofuranose phosphoramidite for DNA synthesis were purchased from Glen Research (Sterling, VA). The crude product was purified by anion-exchange HPLC on a Nucleogen DEAE-60-7 column eluting with a linear gradient from 0 to 1.2 M ammonium acetate in 20% acetonitrile over 60 min at a flow rate of 2 mL/min, and then desalted on a G-10 Sephadex column eluting with deionized water.

Kinetic Studies on DNA Substrates. The rates of DNA hydrolysis and kinetic constants were determined as described previously.[5] Briefly, the depurination reactions were conducted at the pH-optimum of 4.0 and the extent of product release was determined from quantitation of released adenine by HPLC. The steady-state kinetic constants of hydrolysis were calculated directly from the initial reaction rate as a function of substrate concentration by the method of Cornish-Bowden.[19]

Measurement of Kinetic Isotope Effects. A mixture of ^{3}H- and ^{14}C-labeled dA-10 stem-loop molecules, buffered with 10 mM potassium citrate (pH 4.0) and 1 mM EDTA was divided into three portions. The first portion was diluted with 1 mL of solution containing 100 mM ribose in 100 mM potassium phosphate (pH 6.0) and counted to determine the ratio of ^{3}H:^{14}C. In the second portion, depurination was initiated by addition of 0.25 μM RTA at 37 °C and allowed to proceed for approximately 1 h, until 10 to 20% completion. The third portion was incubated at 37 °C for 1 h in the absence of RTA as the background control to detect any radioactive impurity and/or nonspecific hydrolysis of the glycosidic bond of labeled species. To the last two reaction mixtures were added 100 mM Tris·HCl (pH 7.2), 2 mM $Zn(OAc)_2$, 10 mM $MgCl_2$, 0.1 U/μL nuclease P1, 0.004 U/μL snake venom phosphodiesterase, and 0.1 U/μL calf intestinal phosphatase. The resulting mixtures were heated at 37 °C for 5 h, and then passed through small columns of activated charcoal-cellulose (1:4 by weight), and eluted with 100 mM ribose in 100 mM potassium phosphate (pH 6.0). Fractions of eluent (1 mL) were collected and counted for both ^{3}H-labeled and ^{14}C-labeled 2-deoxyribose to determine the KIEs.

Transition-State Modeling. The experimental KIEs indicated a stepwise reaction with formation of an oxocarbenium ion intermediate. Therefore, D_N*A_N[20] or $D_N + A_N$ stepwise mechanisms passing through an oxocarbenium ion intermediate were considered. Because the KIEs were measured by the competitive method,[21] they are KIEs on k_{cat}/K_M. For the stepwise mechanism (eq 1), k_{cat}/K_M is as shown in eq 2.

$$\mathrm{E} + \mathrm{S} \underset{k_2}{\overset{k_1}{\rightleftharpoons}} \mathrm{E{\cdot}S} \underset{k_4}{\overset{k_3}{\rightleftharpoons}} [\mathrm{E{\cdot}O}] \underset{k_6}{\overset{k_5}{\rightleftharpoons}} \mathrm{E{\cdot}P} \xrightarrow{k_7} \mathrm{E} + \mathrm{P} \qquad (1)$$

$$\frac{k_{cat}}{K_M} = \frac{k_1 k_3 k_5 k_7}{k_2 k_4 k_6 \left(1 + \frac{k_7}{k_6}\left(1 + \frac{k_5}{k_4}\left(1 + \frac{k_3}{k_2}\right)\right)\right)} \qquad (2)$$

The observable competitive KIEs will be:

$$\mathrm{KIE} = \frac{\frac{\alpha_1\alpha_3}{\alpha_2}\left(\frac{\alpha_5}{\alpha_4} + \frac{k_5}{k_4}\right)}{1 + \frac{k_5}{k_4}} \qquad (3)$$

where α_n = intrinsic isotope effect on step n.

As shown in eq 3, the experimental KIEs for a stepwise mechanism will depend on k_5/k_4, the ratio that describes the partitioning of the oxocarbenium ion intermediate complex, E·O, forward to products (k_5) or back to reactants (k_4). For all reactions, KIEs on k_{cat}/K_M report on changes between the free substrate plus enzyme in solution (E + S) and the transition state of the *first irreversible step*. In a stepwise mechanism, the ratio k_5/k_4 determines which step is irreversible. If $k_5/k_4 \gg 1$, then essentially all of the intermediate formed, regardless of its lifetime, partitions forward to products. In this case, formation of the intermediate is effectively irreversible and the observable KIE becomes $(\alpha_1\alpha_3)/(\alpha_2)$. This is a D_N‡*A_N mechanism.[22] If $k_5/k_4 \approx 0$, then an equilibrium is established between (E + S) and E·O. Nucleophilic attack of water on the intermediate to give E·P is the irreversible step, making this a D_N*A_N‡ mechanism. In this case, the observable KIE is $(\alpha_1\alpha_3\alpha_5)/(\alpha_2\alpha_4)$. This is the KIE between the free substrate and the transition state for the second chemical step. Alternately, and equivalently, it is the product of the EIE for E·O formation $(\alpha_1\alpha_3)/(\alpha_2\alpha_4)$ and the KIE of E·O breakdown, α_5. At intermediate values of k_5/k_4, there is partitioning of the intermediate in both directions. Both transition states are "partially irreversible" and contribute to the observable KIEs. The values of observable KIEs vary monotonically between the two extrema as a function of k_5/k_4. In the present case, the calculated KIEs at the mechanistic extremes were too similar to each other to use the experimental KIEs to determine k_5/k_4. Therefore, the calculated KIEs for both $k_5/k_4 \gg 1$ and $k_5/k_4 \approx 0$ are reported.

Calculations. All structure optimizations, and energy and frequency calculations were performed using the GAUSSIAN 94 suite of programs,[23] using hybrid density functional theory with Becke's exchange functional[24] and Perdew and Wang's correlation functional,[25] with the 6-31+G** basis set (that is, RB3PW91/6-31+G**), except as noted below. Harmonic frequencies were scaled by 0.956.[26] Fractionation factors were calculated using QUIVER,[27] with the Cartesian force constants scaled by 0.9139 (= 0.956^2). Equilibrium isotope effects (EIEs) were calculated from the fractionation factors as EIE = $\phi_{initial}/\phi_{final}$. KIEs were calculated as KIE = $\phi_{initial}/\phi_{final} \times {}^{light}\nu^*/{}^{heavy}\nu^*$, where ${}^{light}\nu^*$ is the frequency of the imaginary, reaction coordinate, normal mode for the light species.

The isotope effects expected for a stepwise mechanism were calculated quantum mechanically. Stable structures **1**, **3** and **4** were optimized, as well as transition states **2**‡, **5**‡, and **6**‡ (Figure 1). The optimized transition states had one imaginary frequency, the reaction coordinate. Displacement along that normal coordinate resulted in motion of the leaving group/nucleophile toward/away from the electrophilic carbon. Two different transition-state structures for water attack on the oxocarbenium ion (**5**‡) were found. The two transition-state structures were called **5**‡-acute and **5**‡-oblique, based on the H1′−C1′−OH_2 angle (see Supporting Information). The **5**‡-oblique structure involved nucleophile approach from a position that in the full DNA molecule would be close to C4′. Nucleophile attack through **5**‡-oblique would likely be sterically less favorable, therefore the **5**‡-acute structure was chosen for further analysis. Intrinsic reaction coordinate (IRC) calculations were performed on **5**‡-acute and **5**‡-oblique to confirm the correctness of the transition states. In both cases, following the reaction forward to products gives the protonated aldehyde hydrate structure expected for the reaction. Following the reactions backward produced oxocarbenium ion:water complexes with bond lengths of 3.37 and 2.80 Å, respectively, for **5**‡-acute and **5**‡-oblique. Thus, these structures are

(19) Cornish-Bowden, A. *Principles of enzyme kinetics*; Butterworth: London, 1976.

(20) Guthrie, R. D.; Jencks, W. P. *Acc. Chem. Res.* **1989**, *22*, 343−349. In the IUPAC nomenclature, a reaction mechanism is divided into elementary steps, with D_N representing a nucleophilic dissociation and A_N representing a nucleophilic addition. The asterisk indicates that the reaction is stepwise, with a discrete intermediate formed between leaving group departure and nucleophile approach. A bimolecular (S_N2) reaction would be represented as A_ND_N. The asterisk (as distinct from "+") also indicates that the intermediate is too short-lived to diffusionally separate from the leaving group. In an enzyme-catalyzed reaction, the lifetime per se of the intermediate may not be relevant if the leaving group is prevented by enzyme binding from diffusing away. Even if enzyme binding did not prevent diffusional separation, based on the work of Bennet and co-workers[54,55] on 2-deoxy-glucosides, the oxocarbenium ion of DNA is unlikely to be sufficiently long-lived in solution to diffuse away from the enzyme.

(21) Parkin, D. W. In *Enzyme mechanism from isotope effects*; Cook, P. F., Ed.; CRC Press: Boca Raton, 1991; pp 269−290.

(22) The double dagger symbol (‡) indicates which step in the reaction is rate-limiting.

(23) Frisch, M. J.; Trucks, G. W.; Schlegel, H. B.; Gill, P. M. W.; Johnson, B. G.; Robb, M. A.; Cheeseman, J. R.; Keith, T.; Petersson, G. A.; Montgomery, J. A.; Raghavachari, K.; Al-Laham, M. A.; Zakrzewski, V. G.; Ortiz, J. V.; Foresman, J. B.; Cioslowski, J.; Stefanov, B. B.; Nanayakkara, A.; Challacombe, M.; Peng, C. Y.; Ayala, P. Y.; Chen, W.; Wong, M. W.; Andres, J. L.; Replogle, E. S.; Gomperts, R.; Martin, R. L.; Fox, D. J.; Binkley, J. S.; Defrees, D. J.; Baker, J.; Stewart, J. P.; Head-Gordon, M.; Gonzalez, C.; Pople, J. A. *Gaussian 94*, revision C.2, D.4; Gaussian, Inc.: Pittsburgh, PA, 1995.

(24) Becke, A. D. *Phys. Rev. A* **1988**, *38*, 3098−3100.

(25) Perdew, J. P.; Wang, Y. *Phys. Rev. B* **1992**, *45*, 13244.

(26) Wong, M. W. *Chem. Phys. Lett.* **1996**, *256*, 391−399.

(27) Saunders: M.; Laidig, K. E.; Wolfsberg, M. *J. Am. Chem. Soc.* **1989**, *111*, 8989−8994.

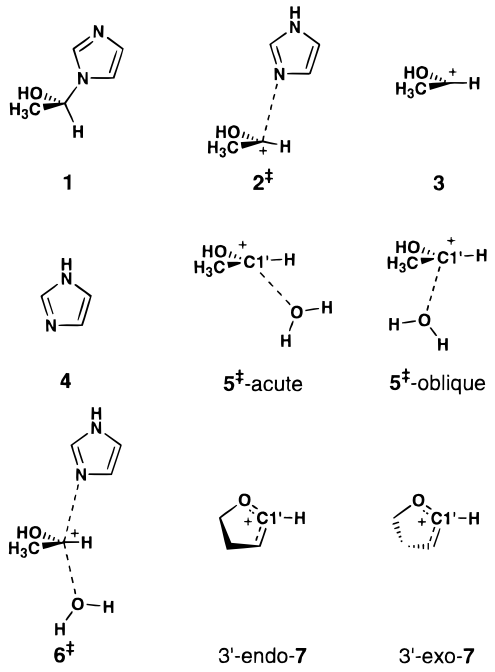

Figure 1. Molecules used in the ab initio analysis for equilibrium and kinetic isotope effects for formation of deoxy-ribooxocarbenium ions and related transition state or equilibrium species. Structures 3′-endo-7 and 3′-exo-7 are enantiomers but are considered as distinct structures because they are models for the oxocarbenium ions in DNA that are not enantiomers due to substituents.

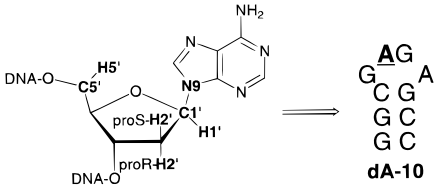

Figure 2. Stem-loop DNA 10-mer containing 2′-deoxy-adenosine residues labeled with ^{3}H,^{14}C, or ^{15}N at the indicated positions (in bold) for kinetic isotope effect measurements. A in underline is the major site of RTA-catalyzed depurination.

the true transition states for nucleophilic attack of water on an oxocarbenium ion. The protonated aldehyde hydrate was analyzed using atoms in molecules (AIM) theory. AIM analysis showed a (3,−1) critical point between the atoms C1′ and O of the water nucleophile. This is the necessary and sufficient condition to state that a bond exists between these two atoms. Thus, the product of nucleophilic attack was a molecule of a protonated aldehyde hydrate, and not merely a hydrated ion complex. The protonated aldehyde hydrate would be a protonated hemiacetal in the full DNA molecule.

Results

Synthesis of Isotopically Labeled DNA. The synthetic procedure of Zimmer and Crothers was followed using isotopically labeled dATP (Figure 2) to prepare DNA 10-mer in quantities sufficient for KIE measurements (Figure 3).[17] The procedure was modified to achieve maximal incorporation of isotopically labeled dATP into the DNA oligomer by lowering the concentration of primer-template. This helps prevent intermolecular self-association of the primer-template and gives yields of 20 to 40%. Labeled dATPs were obtained in high yields (over 90%) through enzymatic reduction of the appropriate ATP precursors by ribonucleoside triphosphate reductase, except [2′R-^{3}H]dATP.

A chemo-enzymatic method was developed for [2′R-^{3}H]-dATP. [2′R-^{3}H]2′-Deoxyadenosine was chemically synthesized

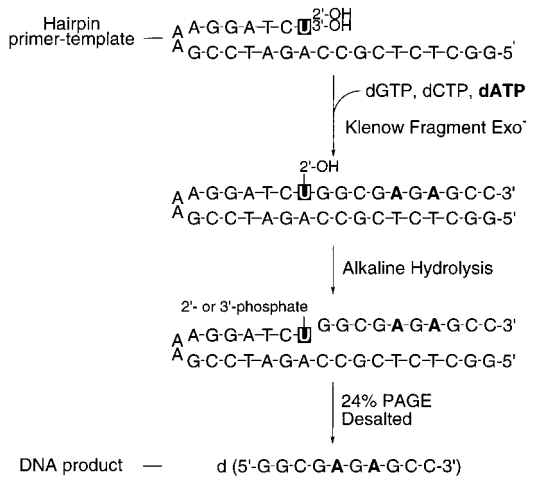

Figure 3. Synthesis of isotopically labeled stem-loop DNA by DNA polymerase-catalyzed primer extension reaction. DNA primer-template and 2′-deoxy-ribonucleotides were used, except for the ribonucleotide residue U (reverse print).

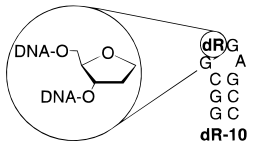

Figure 4. The 1,2-dideoxy-D-ribose-containing (dR) substrate dR-10.

and generously provided by Dr. Hiromi Morimoto of the National Tritium Labeling Facility at Lawrence Berkeley Laboratory using stereoselective reduction of a thioacyl derivative of adenosine with $Bu_3Sn^{3}H$.[28] The ratio of 2′R:2′S ^{3}H-label was determined to be 9:1 by ^{3}H NMR. The observed 2′R-^{3}H KIE was corrected for this ratio. Labeled 2′-deoxyadenosine was mono-phosphorylated at the 5′-position by adenosine kinase, then further converted to the triphosphate by myokinase and pyruvate kinase. Phosphorylation was successful only in the presence of the ATP-regenerating system described in the Methods section. Synthetic DNA 10-mer, called dA-10, was isotopically labeled at specific positions and is shown in Figure 2.

RTA Depurination Site on Stem-Loop DNA Substrate. RTA catalyzes depurination of synthetic stem-loop RNA and DNA molecules containing a GAGA tetraloop motif.[5] The underlined A is the only site depurinated on RNA substrates. The kinetic constants for dA-10 depurination at this site are: k_{cat} = 0.38 min^{-1}, K_M = 2.6 μM, and $k_{cat}/K_M = 3 \times 10^3$ M^{-1}s^{-1}.[5] Prolonged incubation of dA-10 with RTA caused the release of more than one equivalent of adenine, demonstrating that both 2′-deoxyadenosine residues in the DNA tetraloop could be hydrolyzed by RTA. The kinetic constants of depurination at the second site were determined using a DNA 10-mer (dR-10) where the first dA in the d(GAGA) tetraloop was replaced by 1,2-dideoxy-D-ribose (dR in Figure 4). The kinetic parameters for depurination were: $k_{cat}/K_M = 50.8 \pm 3.7$ M^{-1}s^{-1}, $k_{cat} = 0.46 \pm 0.11$ min^{-1} and $K_M = 153 \pm 44$ μM (Figure 5). The maximum substrate concentration of 205 μM, was only slightly higher than K_M. As a result, the value of k_{cat}/K_M was determined with good precision while the errors associated with k_{cat} and K_M individually are higher. The specificity constant, k_{cat}/K_M, for depurination at the second site was 60-fold lower than at the first; therefore, <2% of product formed was from hydrolysis

(28) Robins, M. J.; Wilson, J. S. *J. Am. Chem. Soc.* **1981**, *103*, 932−933.

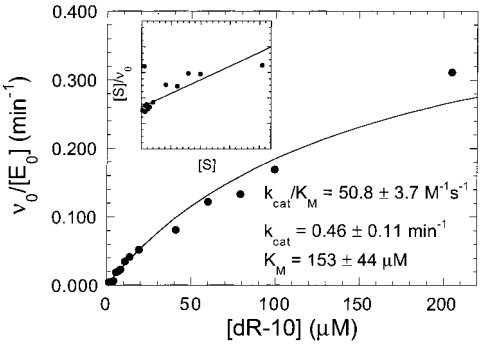

Figure 5. Kinetic constants for RTA-catalyzed depurination of dR-10. A plot of rate vs substrate concentration is shown. (Inset) Hanes plot of $[S]/v_0$ vs [S] for the same data. Kinetic constants were calculated using the method of Cornish-Bowden.[19]

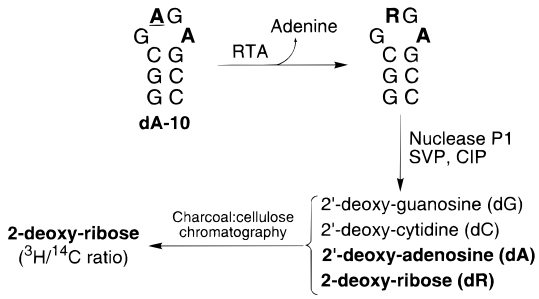

Figure 6. The protocol of kinetic isotope effect measurement on DNA depurination catalyzed by ricin A-chain. Abbreviations: RTA, ricin A-chain; SVP, snake venom phosphodiesterase; CIP, calf intestinal phosphatase.

at the second-site; and it did not interfere significantly with the experimental KIEs.

Kinetic Isotope Effect Measurement. The slow depurination of DNA by RTA made complete depurination of DNA 10-mer impractical. Therefore, KIEs were instead measured by comparison of the ^{3}H/^{14}C ratio in the 2′-deoxyribosyl product of 10% to 20% depurinated DNA with the ratio in intact DNA substrate (Figure 6). Isolation of the 2′-deoxyribosyl group was different from the alkaline treatment of the depurinated RNA[6] because DNA is stable to base. After partial depurination by RTA, the reaction was stopped by neutralizing the pH and the DNA mixture was enzymatically degraded by snake venom phosphodiesterase (SVP), nuclease P1 and calf intestinal phosphatase (CIP) into individual deoxynucleosides, plus 2-deoxyribose from the depurinated site. Deoxyribose was then isolated by charcoal column chromatography and ^{3}H/^{14}C was measured by scintillation counting. The DNA product was resistant to enzymatic degradation when using SVP or nuclease P1 alone, or a mixture of SVP, DNase I and nuclease S1, but it could be cleanly degraded with a combination of SVP and nuclease P1. Nonenzymatic cleavage of glycosidic bonds did not occur in the controls. Calculation of the experimental KIEs was as reported previously.[21] The kinetic isotope effects of DNA depurination catalyzed by RTA are summarized in Table 1.

Discussion

Proposed Mechanism. The experimental KIEs for DNA depurination, like those for RNA depurination,[6] were qualitatively different from those observed for *N*-glycoside hydrolyses determined previously. These KIEs were not consistent with the highly dissociative A_ND_N (S_N2) transition states observed previously, indicating a stepwise $D_N{*}A_N$ mechanism. In particular, the experimental 1′-^{14}C KIE of 1.015 ± 0.001 was lower than the minimum KIE possible for an A_ND_N mechanism, 1.025, as calculated using the bond order vibrational analysis method,[29,30] and 1.029 as calculated for the reaction of **1** to **6**‡ by ab initio methods. In contrast, 1′-^{14}C KIEs as low as 1.010 are possible with a $D_N{*}A_N$ mechanism (Table 2). The unusually low 1′-^{14}C KIE for DNA depurination can only be explained by proposing a $D_N{*}A_N$ mechanism for the DNA depurination reaction. Therefore, RTA is proposed to catalyze a stepwise formation of a discrete enzyme·oxocarbenium ion intermediate (E·O) before conversion to products (Figure 7).[20]

Table 1. Kinetic Isotope Effects on DNA Depurination Catalyzed by Ricin A-Chain

labeled dA-10	type of KIE	experimental KIEs[a]
[1′-^{14}C],[5′-^{3}H]	primary ^{14}C	1.015 ± 0.001 (3)[b]
[9-^{15}N, 5′-^{14}C],[5′-^{3}H]	primary ^{15}N	1.023 ± 0.004 (3)[b]
[1′-^{3}H],[5′-^{14}C]	α-secondary ^{3}H	1.187 ± 0.008 (4)
[2′S-^{3}H],[5′-^{14}C]	β-secondary ^{3}H	1.117 ± 0.002 (2)
[2′R-^{3}H],[5′-^{14}C]	β-secondary ^{3}H	1.146 ± 0.008 (5)[c]
[5′-^{3}H],[5′-^{14}C]	δ-secondary ^{3}H	1.014 ± 0.004 (3)

[a] The number in parentheses is the number of independent KIE experiments. [b] KIEs were corrected for the 5′-^{3}H KIE according to the expression: $KIE_{experimental} = KIE_{observed} \times [5'\text{-}^3H]$. [c] Value corrected for presence of 10% 2′S-^{3}H.

The reactions of RTA with RNA[6] and DNA stand in contrast to the transition states for all *N*-riboside hydrolysis reactions previously studied in this laboratory, which all proceed through highly dissociative A_ND_N mechanisms.[7,16,31−42] The fact that so many other hydrolase enzymes catalyze concerted A_ND_N reactions implies that the ribooxocarbenium and deoxy-ribooxocarbenium ions are very unstable and that some unique feature of the RTA structure stabilizes a discrete intermediate. Any such interactions are not apparent in the X-ray crystal structures of RTA cocrystallized with substrate analogues or weak inhibitors bound.[43,44] Attempts to cocrystallize RTA with stem-loop RNA analogues containing features of the transition state are continuing. Dramatic changes were observed in the structures of a nucleoside hydrolase and phosphoribosyl transferases when cocrystallized with transition-state inhibitors.[45−47]

(29) Berti, P. J. *Methods Enzymol.* **1999**, *308*, 355−397.
(30) Sims, L. B.; Lewis, D. E. In *Isotope Effects: Recent Developments in Theory and Experiment*; Buncel, E., Lee, C. C., Eds.; Elsevier: New York, 1984; Vol. 6, pp 161−259.
(31) Scheuring, J.; Berti, P. J.; Schramm, V. L. *Biochemistry* **1998**, *37*, 2748−2758.
(32) Scheuring, J.; Schramm, V. L. *Biochemistry* **1997**, *36*, 8215−8223.
(33) Scheuring, J.; Schramm, V. L. *Biochemistry* **1997**, *36*, 4526−4534.
(34) Berti, P. J.; Blanke, S. R.; Schramm, V. L. *J. Am. Chem. Soc.* **1997**, *119*, 12079−12088.
(35) Berti, P. J.; Schramm, V. L. *J. Am. Chem. Soc.* **1997**, *119*, 12069−12078.
(36) Rising, K. A.; Schramm, V. L. *J. Am. Chem. Soc.* **1997**, *119*, 27−37.
(37) Kline, P. C.; Schramm, V. L. *Biochemistry* **1995**, *34*, 1153−1162.
(38) Kline, P. C.; Schramm, V. L. *Biochemistry* **1993**, *32*, 13212−13219.
(39) Horenstein, B. A.; Parkin, D. W.; Estupinan, B.; Schramm, V. L. *Biochemistry* **1991**, *30*, 10788−10795.
(40) Parkin, D. W.; Mentch, F.; Banks, G. A.; Horenstein, B. A.; Schramm, V. L. *Biochemistry* **1991**, *30*, 4586−4594.
(41) Parkin, D. W.; Schramm, V. L. *Biochemistry* **1987**, *26*, 913−920.
(42) Parkin, D. W.; Schramm, V. L. *J. Biol. Chem.* **1984**, *259*, 9418−9425.
(43) Yan, X.; Hollis, T.; Svinth, M.; Day, P.; Monzingo, A. F.; Milne, G. W.; Robertus, J. D. *J. Mol. Biol.* **1997**, *266*, 1043−1049.
(44) Weston, S. A.; Tucker, A. D.; Thatcher, D. R.; Derbyshire, D. J.; Pauptit, R. A. *J. Mol. Biol.* **1994**, *244*, 410−422.
(45) Degano, M.; Almo, S. C.; Sacchettini, J. C.; Schramm, V. L. *Biochemistry* **1998**, *37*, 6277−6285.
(46) Shi, W. X.; Li, C. M.; Tyler, P. C.; Furneaux, R. H.; Grubmeyer, C.; Schramm, V. L.; Almo, S. C. *Nat. Struct. Biol.* **1999**, *6*, 588−593.
(47) Shi, W. X.; Li, C. M.; Tyler, P. C.; Furneaux, R. H.; Cahill, S. M.; Girvin, M. E.; Grubmeyer, C.; Schramm, V. L.; Almo, S. C. *Biochemistry* **1999**, *38*, 9872−9880.

Table 2. Calculated Fractionation Factors and Isotope Effects for Hydrolysis of a Model *N*-Glycoside

		$2^{‡}$				$5^{‡}$-acute				observable KIEs		
isotopic label	**1** ϕ^a	ϕ	rxn coord[b]	**3** ϕ	**4** ϕ	ϕ	rxn coord	EIE[c] **1** ↔ **3**+**4**	KIE[d] **3** → $\mathbf{5}^{‡}$	$D_N{*}A_N{}^{‡}$ ($k_5/k_4 \approx 0$)[e]	$D_N{}^{‡}{*}A_N$ ($k_5/k_4 \gg 1$)[f]	experimental KIEs[g]
1′-^{14}C	1.311	1.306	1.015	1.312		1.311	1.011	0.999	1.011	1.010	1.018	1.015
9-^{15}N	1.118	1.093	1.005		1.092			1.024	1[h]	1.024	1.028	1.023
1′-^{3}H	34.374	22.364	1.224	26.528		26.765	1.065	1.296	1.056	1.368	1.882	1.187
2′S-^{3}H	23.875	20.540	1.109	19.691		21.105	1.008	1.212	0.941	1.140	1.289	1.117
2′R-^{3}H	24.434	20.312	1.086	19.754		16.901	1.062	1.237	1.241	1.535	1.306	1.146

[a] ϕ = fractionation factors. [b] rxn coord = $^{light}\nu^{*}/^{heavy}\nu^{*}$ = contribution from reaction coordinate (imaginary) frequency. [c] EIE(**1** ↔ **3** + **4**) = $\phi\mathbf{1}/\phi\boldsymbol{x}$, where $\boldsymbol{x}$ = **3** or **4**. [d] KIE(**3** → $\mathbf{5}^{‡}$-acute) = $\phi\mathbf{3}/\phi\mathbf{5}^{‡}$-acute·($^{light}\nu^{*}/^{heavy}\nu^{*})_{5^{‡}-acute}$. [e] KIE = EIE(**1** ↔ **3** + **4**)·KIE(**3** → $\mathbf{5}^{‡}$-acute). [f] KIE(**1** → $\mathbf{2}^{‡}$) = $\phi\mathbf{1}/\phi\mathbf{2}^{‡}$·($^{light}\nu^{*}/^{heavy}\nu^{*})_{2^{‡}}$. [g] Experimental KIEs from Table 1. [h] The leaving group does not undergo change in this step, so the KIE is 1 by definition.

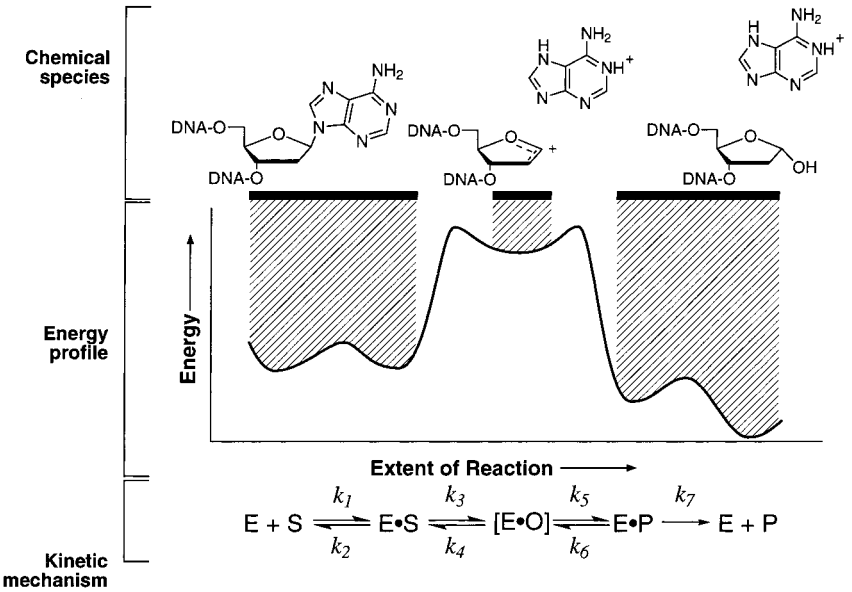

Figure 7. Chemical and kinetic mechanism of RTA-catalyzed DNA hydrolysis. In the proposed mechanism, departure of the adenine leaving group forms a discrete oxocarbenium ion intermediate complexed with the enzyme. In a separate step, the intermediate undergoes nucleophilic attack from water to form products. The adenine ring is shown protonated at N1 and N7, by analogy to the RNA reaction.[6] There is no direct evidence in the DNA reaction for the protonation state of the adenine ring. (upper panel) The chemical species present at each stage of the mechanism is indicated by the hatched areas. (middle panel) A schematic representation of the changes in the course of the reaction. (bottom panel) The kinetic mechanism: E, free enzyme in solution, S, free substrate, E·S, Michaelis complex, E·O, enzyme·(oxocarbenium ion + adenine) complex, E·P, enzyme·products complex, P, free products in solution; k_n, rate constant on step n.

Agreement with ab Initio Calculated KIEs: Primary 1′-^{14}C and 9-^{15}N KIEs. KIEs calculated for small model compounds using ab initio methods gave a reasonably good match to the experimental KIEs (Table 2). The calculated primary 1′-^{14}C KIEs for both the $D_N{}^{‡}{*}A_N$ (1.010) and $D_N{*}A_N{}^{‡}$ (1.018) mechanisms were in reasonably good agreement with the experimental 1′-^{14}C KIE (1.015). The calculated primary 9-^{15}N KIEs for both the $D_N{}^{‡}{*}A_N$ (1.028) and $D_N{*}A_N{}^{‡}$ (1.024) mechanisms were also in good agreement with the experimental KIE (1.023).

The calculated KIEs for the two mechanistic extremes of $D_N{}^{‡}{*}A_N$ and $D_N{*}A_N{}^{‡}$ are not different enough from each other to be able to distinguish whether the experimental KIEs are more consistent with one than the other. The calculated 2′S-^{3}H KIE supports a $D_N{*}A_N{}^{‡}$ mechanism (see below). However, it is not clear that this computed value is reliable enough to be used on its own to distinguish between the mechanistic extremes. Considering the experimental KIEs for the RTA-catalyzed depurination of both RNA and DNA reactions together, the balance of evidence favors a $D_N{*}A_N{}^{‡}$ mechanism. The RNA reaction involves formation of an equilibrium population of oxocarbenium ion intermediate followed by a rate-limiting, nonchemical step. This implies that RTA is also capable of forming an equilibrium population of the deoxy-oxocarbenium ion intermediate before nucleophilic attack. Thus, a $D_N{*}A_N{}^{‡}$ mechanism is favored for depurination of DNA by RTA.

1′-^{3}H KIE. The experimental 1′-^{3}H KIE was 1.187. This is consistent with α-secondary ^{3}H KIEs determined for related *N*-riboside hydrolyses.[7,16,31−42] As has been observed previously,[6,32] the 1′-^{3}H KIEs calculated by ab initio methods (1.368 for $D_N{*}A_N{}^{‡}$, 1.882 for $D_N{}^{‡}{*}A_N$) are larger than any experimental KIE for this reaction.[6,31] Although the source of the computational discrepancy is poorly understood, it does not influence the transition-state determination for KIEs at other positions because it is possible to adjust the bending force constants involving H1′ to bring the KIEs calculated by bond energy/bond order vibrational analysis[29,30] into agreement with the experimental KIE without changing other features of the transition-state structure.

Stereospecific 2′-^{3}H KIEs. The 2′S-^{3}H KIE calculated for a $D_N{*}A_N{}^{‡}$ mechanism (1.140) is in good agreement with the experimental KIE (1.117), in contrast to the calculated $D_N{}^{‡}{*}A_N$ KIE (1.289). The calculated KIE for a $D_N{*}A_N{}^{‡}$ mechanism arises from a large, normal contribution of 1.212 for the equilibrium formation of the oxocarbenium ion, followed by an inverse contribution of 0.940 for the nucleophilic attack of water. The normal EIE on oxocarbenium ion formation results from hyperconjugation between the C2′−H2′ bonds with the p-orbital

of C1′.[48] Upon nucleophilic attack, C1′ becomes rehybridized from sp^2 toward sp^3. The loss of hyperconjugation leads to a shorter C2′−H2′S bond and an inverse KIE on that step. Similarly the 2′R-^{3}H EIE on oxocarbenium ion formation is large and normal at 1.237. Unexpectedly, the KIE calculated for water nucleophilic attack is also large and normal (1.241), leading to the very large calculated observable KIE of 1.535. This appears to be an artifact of the density functional theory optimization of the transition-state structure. A more reasonable estimate of the 2′R-^{3}H based on MP2 optimizations would be approximately 1.2 (see Supporting Information).

Structure of the d(GAGA) Tetraloop and Ribosyl Ring Conformation. Unlike the RNA case, there are no X-ray or NMR structures available for a DNA tetraloop with the RTA-specific sequence. However, an NMR structure of DNA containing the sequence d(GTTA) in a tetraloop structure has been determined,[49] and the backbone trace is similar to the RNA structures.[50,51] Residue dT9 is the second residue of the tetraloop structure d(GTTA), located in a position analogous to the depurination site of dA-10, d(GAGA). The ribosyl ring of dT9 adopts a 2′-endo[52] conformation in the NMR-derived structure, compared with 3′-endo in RNA. The 2′-endo conformation is not stable in model compound **7** of the oxocarbenium ion. It spontaneously changes into a 3′-exo conformation. The only other stable ring conformation for the oxocarbenium ion is 3′-endo. In the optimized structures of both 3′-endo- and 3′-exo-**7**, near-optimal hyperconjugation between the p-orbital of C1′ and the two C2′−H2′ bonds is achieved (Figure 8). This high degree of hyperconjugative stabilization is reflected in the experimental KIEs of >1.1, as compared with the RNA substrate with its weak hyperconjugation and low experimental 2′-^{3}H KIE of 1.012. In principle, it should be possible to determine the ribosyl ring conformation from the relative magnitudes of the 2′S-^{3}H and 2′R-^{3}H KIEs.[53] However, it is likely that the presence of the nucleophile will influence the 2′R-^{3}H KIE more than the 2′S-^{3}H KIE (see Supporting Information). Thus, it is not possible to determine the exact geometry of the deoxyribose ring. However, the large and nearly equal 2′S- and 2′R-^{3}H KIEs strongly support substantial orbital overlap with both β-hydrogens as summarized in Figure 8.

The structural constraints on forming an oxocarbenium ion are less stringent for DNA than RNA. Both 3′-exo- and 3′-endo-2′-deoxy-ribooxocarbenium ions can be superimposed with residue dT9 of the NMR-derived d(GTTA) tetraloop structure without large-scale changes in ribosyl ring position or distortion to the nucleotide backbone (Figure 9). In contrast, the equivalent analysis with RNA oxocarbenium ions demonstrated that only the 3′-endo conformation of the oxocarbenium ion could be accommodated.[6] The relative adaptability of the 2′-deoxy-ribooxocarbenium ion structure allows hyperconjugative stabilization of the oxocarbenium ion to determine the ring conformation, thereby increasing its stability and decreasing the energetic barrier to its formation.

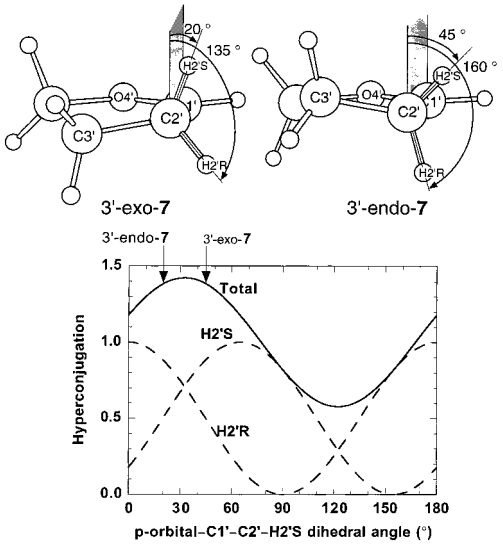

Figure 8. Hyperconjugation in optimized oxocarbenium ion model compounds. (Above) Optimized structures 3-endo-**7** and 3-exo-**7** showing p-orbital-C1′−C2′−H2′ dihedral angles. (Below) Angular dependence of hyperconjugation. Overall hyperconjugative stabilization is the sum of the individual components and is shown (—) as a function of dihedral angle. The individual contributions from H2′S and H2′R (− − −) are also shown. The angular dependence of hyperconjugation is given by: hyperconjugation $\propto \exp(\cos^2 \theta)$, where θ is the dihedral angle defined by p-orbital−C1′−C2′−H2′.[53]

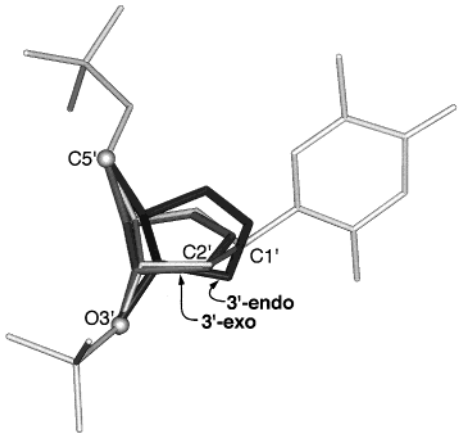

Figure 9. Oxocarbenium ion conformation. The NMR structure[49] of residue dT9 (light gray) of a d(GTTA) tetraloop is superimposed with quantum mechanically optimized deoxy-ribooxocarbenium ion structures in 3′-exo (medium gray) and 3′-endo (dark gray) conformations.

DNA versus RNA Substrates. The use of DNA as an alternate substrate allows features of the chemical mechanism to be observed via KIEs that were masked in the A-10 RNA reaction. Specifically, while the RNA reaction included an isotopically insensitive rate-limiting step that obscured the KIEs of the attack of water on the ribooxocarbenium, the KIEs for the DNA reaction arise from the intrinsic chemical KIEs. Observing the intrinsic chemical KIEs of a stepwise mechanism for the DNA reaction further support the interpretation of the RNA KIEs as involving a nonchemical step.[6] The change in mechanism is also reflected by the changes in kinetic rate constants. The k_{cat} for dA-10 is 0.38 min^{-1}, compared with 4 min^{-1} for A-10. This 10-fold reduction in k_{cat} causes the chemical steps to become rate-limiting. The slow chemistry

(48) Hehre, W. J. *Acc. Chem. Res.* **1975**, *8*, 369−376; *Adv. Carbohydr. Chem. Biochem.* **2000**, *55*, 265−310.

(49) van Dongen, M. J.; Mooren, M. M.; Willems, E. F.; van der Marel, G. A.; van Boom, J. H.; Wijmenga, S. S.; Hilbers, C. W. *Nucleic Acids Res.* **1997**, *25*, 1537−1547.

(50) Correll, C. C.; Munishkin, A.; Chan, Y. L.; Ren, Z.; Wool, I. G.; Steitz, T. A. *Proc. Natl. Acad. Sci. U.S.A.* **1998**, *95*, 13436−13441.

(51) Jucker, F. M.; Heus, H. A.; Yip, P. F.; Moors, E. H.; Pardi, A. *J. Mol. Biol.* **1996**, *264*, 968−980.

(52) Altona, C.; Sundaralingam, M. *J. Am. Chem. Soc.* **1972**, *94*, 8205−8211. In the 3′-endo conformation, all other atoms in the ribosyl ring (C1′, C2′, C4′, O4′) are coplanar, with C3′ "above" the plane of the ring. That is, it is on the same side as the adenine ring substituent at C1′. In the 3′-exo conformation, C3′ is "below" the plane or the ribosyl ring. See Figure 8.

(53) Sunko, D. E.; Szele, I.; Hehre, W. J. *J. Am. Chem. Soc.* **1977**, *99*, 5000−5004.

(54) Zhu, J.; Bennet, A. J. *J. Am. Chem. Soc.* **1998**, *120*, 3887−3893.

(55) Huang, X. C.; Tanaka, K. S. E.; Bennet, A. J. *J. Am. Chem. Soc.* **1997**, *119*, 11147−11154.

could be the result of one or more effects: (1) Decreased specificity for the substrate leads to a decreased rate of formation and stabilization of the oxocarbenium ion intermediate. (2) The increased stability of the deoxy-ribooxocarbenium ion may make it sufficiently long-lived that the chemical step of nucleophilic attack, as distinct from simple diffusion of the nucleophile into position for attack, becomes rate-limiting. As discussed previously,[6] the 2′-deoxy-ribooxocarbenium ion is approximately 3.8 kcal/mol more stable than the 2′-hydroxy-ribooxocarbenium ion. (3) The rate-limiting, isotopically insensitive step in RNA hydrolysis becomes faster in the DNA reaction and is no longer rate-limiting. It is not possible to distinguish between these mechanistic possibilities from the available data, although one of the first two mechanisms, or a combination of them, seems more probable.

The experimental KIEs reflect the chemical steps of dA-10 hydrolysis and represent the first determination of a $D_N{*}A_N$ stepwise mechanism for hydrolysis of a ribofuranoside. The reactions of both RNA and DNA with RTA proceed through distinctly different mechanisms from the nonenzymatic reaction. Acid-catalyzed AMP hydrolysis proceeds through a concerted A_ND_N (S_N2) transition state involving simultaneous approach of the nucleophile and departure of the leaving group. No discrete oxocarbenium ion intermediate is formed.[7] The change in reaction mechanism indicates that RTA uses binding energy from enzyme·substrate interactions to stabilize a discrete oxocarbenium ion intermediate. Details of precisely how this is accomplished await an X-ray crystal structure of a RTA· transition-state inhibitor complex; however, certain general themes are clear. First, enzymatic protonation of the adenine-leaving group, certainly at N7 and probably at N1, is necessary to avoid forming the highly nucleophilic adenine anion.[6] The change in structure and charge distribution on forming the oxocarbenium ion can also be used by the enzyme in stabilizing the intermediate.

Conclusions

RTA-catalyzed hydrolysis of dA-10 proceeds through a $D_N{*}A_N$ stepwise mechanism that involves formation of a discrete enzyme·deoxy-ribooxocarbenium ion complex before nucleophilic attack by water in a separate step. RTA-catalyzed hydrolysis is unique because it is the first instance where stepwise hydrolytic mechanisms of ribofuranosides have been observed. The DNA reaction is also unique because the intrinsic chemical steps are expressed in the KIEs and not obscured by nonchemical steps, as in the case of RNA depurination. The DNA transition-state structure was valuable in interpreting the KIEs for the RNA hydrolysis reaction described previously and has helped elucidate details of the hydrolytic mechanism. In the future, it will be helpful in designing transition-state inhibitors of RTA.

Acknowledgment. This work was supported by NIH Research Grant CA72444. We gratefully acknowledge Dr. Hiromi Morimoto of the National Tritium Labeling Facility at Lawrence Berkeley Lab for the generous gift of [2′R-^{3}H]2′-deoxyadenosine, Dr. Joanne Stubbe of the Massachusetts Institute of Technology for the gift of the overexpression system for ribonucleoside triphosphate reductase, and Dr. Piotr Paneth of the Technical University of Lodz for helpful discussions on the derivation of eqs 2 and 3.

Supporting Information Available: A further discussion of computationally optimized structures and 2′-^{3}H KIEs is available in the Supporting Information (PDF). Also available are *Z*-matrices of compounds **1** through **7** (ASCII and PDF) and calculated KIEs for additional structures, including **5**‡-oblique (PDF). This material is available free of charge via the Internet at http://pubs.acs.org.

JA992751A